Proc. Natl. Acad. Sci. USA
Vol. 92, pp. 11824–11828, December 1995
Biochemistry

MyoD forms micelles which can dissociate to form heterodimers with E47: Implications of micellization on function

(analytical ultracentrifugation/helix–loop–helix proteins/transcriptional regulation)

THOMAS M. LAUE[†‡], MELISSA A. STAROVASNIK[§¶], HAROLD WEINTRAUB[‖††], XIAO-HONG SUN[‡‡], LAUREN SNIDER[‖], AND RACHEL E. KLEVIT[§]

[†]Department of Biochemistry and Molecular Biology, Life Sciences Building, University of New Hampshire, Durham, NH 03824-3544; [§]Department of Biochemistry, SJ-70, University of Washington, Seattle, WA 98195; [‖]Howard Hughes Medical Institute, Fred Hutchinson Cancer Research Center, 1124 Columbia Street, Seattle, WA 98104; and [‡‡]Department of Cell Biology, New York University Medical Center, New York, NY 10016

Communicated by Howard Schachnan, University of California, Berkeley, CA, July 24, 1995 (received for review May 15, 1995)

ABSTRACT **MyoD is a member of a family of DNA-binding transcription factors that contain a helix–loop–helix (HLH) region involved in protein–protein interactions. In addition to self-association and DNA binding, MyoD associates with a number of other HLH-containing proteins, thereby modulating the strength and specificity of its DNA binding. Here, we examine the interactions of full-length MyoD with itself and with an HLH-containing peptide portion of an E2A gene product, E47-96. Analytical ultracentrifugation reveals that MyoD forms micelles that contain more than 100 monomers and are asymmetric and stable up to 36°C. The critical micelle concentration increases slightly with temperature, but micelle size is unaffected. The micelles are in reversible equilibrium with monomer. Addition of E47-96 results in the stoichiometric formation of stable MyoD–E47-96 heterodimers and the depletion of micelles. Micelle formation effectively holds the concentration of free MyoD constant and equal to the critical micelle concentration. In the presence of micelles, the extent of all interactions involving free MyoD is independent of the total MyoD concentration and independent of one another. For DNA binding, the apparent relative specificity for different sites can be affected. In general, heterodimer-associated activities will depend on the self-association behavior of the partner protein.**

Implicit in all current models of gene regulation are thermodynamic linkages between protein–protein association and protein–DNA binding. Proteins containing the basic helix–loop–helix (bHLH) motif require oligomerization to form either homomeric or heteromeric complexes with high-affinity DNA-binding activity (1–3). These proteins regulate gene expression by binding to DNA containing the consensus E-box sequence CANNTG (2, 4, 5). The HLH region is responsible for protein dimerization, and the basic region is directly involved in DNA binding (3, 6–10).

MyoD is a transcriptional activator that plays a principal role in muscle differentiation (11, 12). It is one of a family of bHLH-containing muscle determination/differentiation factors that appear to function *in vivo* as heteromers with E2A gene products E12 and E47 (13, 14). A 68-residue peptide containing the bHLH region of MyoD is sufficient for conversion of fibroblasts to myoblasts (15). The bHLH region of MyoD (MyoD-bHLH) forms dimers and tetramers in the absence of DNA (16) and binds DNA as a dimer (10).

The oligomeric states of full-length myogenin, MyoD, and E12 have been assessed by using thin-zone sucrose-gradient sedimentation (17). These studies demonstrate that in the absence of DNA both myogenin and MyoD reversibly form oligomers larger than dimer size and that E12 predominantly forms dimers. However, the reequilibration between oligomeric forms during the course of these experiments made it difficult to ascertain the stoichiometries.

To obtain direct evidence about the association behavior of MyoD, analytical ultracentrifugation experiments have been carried out on full-length MyoD, both alone and mixed with an HLH-containing peptide of E47 (E47-96). MyoD exhibits micellular behavior—i.e., highly cooperative and reversible self-association—forming asymmetric assemblies containing more than 100 monomers. Such behavior could have significant implications for the function of MyoD.

MATERIALS AND METHODS

MyoD Preparation. Full-length MyoD and MyoD-bHLH were expressed and purified as described (16, 18). The protein (≈1 mg) was size fractionated on a Superose 6 column by using a Pharmacia fast protein liquid chromatography (FPLC) system. The column running buffer was 10% (vol/vol) glycerol/20 mM Hepes, pH 7.6/2 mM EDTA/0.1% Triton X-100/0.1 M NaCl/1 mM dithiothreitol/1 mM phenylmethylsulfonyl fluoride/2 μg each of pepstatin and leupeptin per ml. Fractions (0.2 ml) were collected, and aliquots were analyzed by a gel mobility-shift assay. Electrophoretic mobility-shift assays were performed essentially as described (18–20) by using 5% miniacrylamide gels. Purified protein was incubated for 5 min at room temperature in 20 mM Hepes, pH 7.6/50 mM KCl/3 mM $MgCl_2$/1 mM EDTA/0.5% Nonidet P-40 with 500 ng of an oligonucleotide probe containing the muscle creatine kinase (MCK) enhancer-binding sites for MyoD.

E47-96 Construction, Expression, and Purification. A phage T7 RNA polymerase-driven expression plasmid (21) encoding the fragment of E47 containing the bHLH region (residues 317–413, numbered as described in ref. 1) was constructed in the pRSET A vector (Invitrogen). BL21(DE3) cells containing the pLysS plasmid (22) were transformed with this plasmid to produce E47-96. The resultant protein included an Ala-Arg dipeptide at the N terminus and a Met at the C terminus. Cells were grown at 37°C on minimal medium to an OD_{650} of 0.8, then induced with 1 mM isopropyl β-D-thiogalactoside and harvested 4 h later. Protein purification was essentially as described for MyoD-bHLH (16), except lower salt concentrations were used for lysis and cation-exchange chromatography. Cells were lysed by cycles of freezing and thawing in the presence of 50 mM Hepes, pH 7.6/1 mM EDTA/1 mM $MgCl_2$, 0.1% Triton X-100/5 mM dithiothreitol/1 mM phenylmethylsulfonyl fluoride. Crude cell extract was loaded onto an SP Sepharose column

The publication costs of this article were defrayed in part by page charge payment. This article must therefore be hereby marked "*advertisement*" in accordance with 18 U.S.C. §1734 solely to indicate this fact.

Abbreviations: HLH, helix–loop–helix; bHLH, basic HLH; cmc, critical micelle concentration; MyoD-bHLH, bHLH region of MyoD.

[‡]To whom reprint requests should be addressed.
[¶]Present address: Department of Protein Engineering, Genentech, Inc., South San Francisco, CA 94080.
[††]Deceased, March 28, 1995.

(Pharmacia) pre-equilibrated in 50 mM Hepes, pH 7.6/1 mM dithiothreitol/1 mM EDTA/1 mM phenylmethylsulfonyl fluoride. E47-96 eluted when the NaCl concentration reached ≈0.2 M in a linear NaCl gradient. Final purification by HPLC (>95%) was as described (16). Electrospray mass spectrometry (m = 11,533) revealed that E47-96 lacked the N-terminal methionine.

Analytical Ultracentrifugation. Samples were dialyzed exhaustively against 50 mM Tris/25 mM acetate, pH 7.2/100 mM NaCl. Short column equilibrium sedimentation (23) was carried out at 23.3°C in a Model E analytical ultracentrifuge equipped with an on-line Rayleigh optical system (24). Data were edited and analyzed as described (25). Yielding z-average reduced molecular weights, σ_z (ref. 26; where $\sigma_z \equiv \Sigma\, c_i\sigma_i 2/\Sigma\, c_i\sigma_i$, with c_i the mass concentration and σ_i the reduced molecular weight of the ith component). Molecular weights (M_z) were calculated from σ_z by using a measured buffer density of 1.004 g/ml (23.3°C). Partial specific volumes ($\bar{\nu}$) for MyoD (0.71_8 ml/g), MyoD-bHLH (0.72_5 ml/g), and E47-96 (0.73_1 ml/g) were calculated from their amino acid compositions and adjusted by −0.028 ml per gram of MyoD-bHLH E47-96 and −0.014 ml per gram of E47-96 to account for electrostriction effects (27, 28). An additional error of ±0.015 in $\bar{\nu}$ was included in calculating the confidence interval of M_z. No charge correction was applied to the $\bar{\nu}$ of MyoD.

The critical micelle concentration (cmc) was estimated from the baseline-corrected A_{280} of the slowest boundary (<6 s) in sedimentation velocity experiments, using a calculated ε_{280} of 0.48 ml·mg^{-1}·cm^{-1}. The cmc determined in this fashion should be considered a low estimate since dissolution of the micelles at faster boundaries will contribute to the absorbance in the slower boundary.

Sedimentation velocity was conducted using a four-hole titanium rotor at 10,000, 20,000, 48,000, and 60,000 rpm and at a constant temperature of 20.0°C or 36.0°C. Absorbance profiles were obtained at 280 nm in the XL-A analytical ultracentrifuge by using 12-mm-thick, aluminum-filled or carbon-filled epon centerpieces and fused silica windows. Integral sedimentation coefficient distributions, $G(s^*)$, were determined from individual scans, and differential sedimentation coefficient distributions, $g(s^*)$, were determined as described by Stafford (29). No attempt was made to correct for the effects of diffusion. Correction of the sedimentation coefficients to standard conditions was done as described (26).

RESULTS

Analytical Ultracentrifugation of MyoD. Equilibrium sedimentation analyses of MyoD (monomer M_r = 34,300; predicted charge, −6e) at rotor speeds below 5000 rpm (Table 1) reveals that it forms large aggregates ($M_z \approx 4\text{–}5 \times 10^6$) consisting of approximately 120 monomers. At 10,000 rpm there was no discernable fringe displacement, except at the very bottom of the cell, and no fringe displacement could be detected at 20,000 rpm. These observations indicate that the concentration of dissociated MyoD was ≲600 nM at 23.3°C. The aggregates are somewhat heterogeneous in size, as evidenced by the decrease in M_z with increasing rotor speed (Table 1). It is unlikely that this decrease reflects a pressure-induced dissociation. There was no systematic concentration-dependence of M_z, precluding an examination of mass-action behavior.

Sedimentation velocity was used to examine the particle size distribution, to estimate the concentration of small oligomers (Fig. 1), and to determine whether or not the aggregates are stable at elevated temperatures (Fig. 2). At 20°C, over 95% of the material (0.58 A_{280}, initial concentration) is in a slightly-skewed boundary at 50 s (Fig. 1), again indicating that the micelles do not have a discrete upper size limit. The lack of material intermediate to the faster and slower sedimenting boundaries (Fig. 1A) indicates that any association is highly cooperative. Of the remaining 5%, only half (≈0.01 A_{280}) sedimented at 48,000 rpm, moving at about 3–4 s. The size of the 3- to 4-s material is uncertain, but it is likely to be smaller than a tetramer. On the basis of the corrected absorbance around 6S, the concentration of small oligomers is ≈600 nM, in accord with the earlier result (above).

Table 1. Sedimentation equilibrium of MyoD, E47-96, and 1:1 complex of full-length MyoD–E47-96

Protein	M_r, $\times 10^{-3}$	rms fringes*
MyoD†		
2200 rpm	5010 (4840, 5180)	0.018
3200 rpm	4120 (4050, 4190)	0.019
4400 rpm	3860 (3770, 3940)	0.03
2200, 3200, and 4400 rpm	4090 (4040, 4140)	0.024
E47-96‡	22.9 (22.3, 23.5)	0.012
MyoD:E47-96§	47.0 (45.0, 49.0)	0.024
MyoD-bHLH–E47-96¶	20.2 (19.5, 20.9)	0.021

*rms of the variance of the nonlinear least-squares fit. Fringe displacement concentration units can be converted to mg/ml by dividing by 3.52.

†All values are based on the simultaneous fit of data acquired at concentrations of 1.8, 1.2, 0.72, 0.36, and 0.18 mg/ml and rotor speeds listed.

‡Values are based on the simultaneous fit of data acquired at concentrations of 0.9, 0.65, 0.4, and 0.2 mg/ml and at rotor speeds of 20,000, 28,000, and 36,000 rpm.

§A 1:1 molar mixture of MyoD and E47-96. Values are based on the simultaneous fit of data acquired at concentrations of 1.4, 0.92, 0.46, and 0.23 mg/ml and at rotor speeds of 20,000, 28,000, and 36,000 rpm.

¶Equimolar mixtures of MyoD-bHLH and E47-96 were examined at 4.5, 2.3, 1.2, 0.59, 0.32, and 0.16 mg/ml and at rotor speeds of 20,000, 38,000, and 36,000 rpm. It was not possible to determine the nonideality for this complex, and the value presented here was determined assuming B = 0. When a realistic estimate of the second virial coefficient was included (BM = 6 ml/g) the apparent molecular weight rose to 20,500.

The micelles are stable at 36°C, as shown in Fig. 2. Over 67% of the material moved at ≈80 s^*, and 30% moved at ≈5 s^*. The well-defined plateau region above 90 s^* indicates that the micelles have a discrete upper size limit at this temperature. When s^* is adjusted to standard conditions, the micelles sediment at $s_{20,w}$ = 50, indicating that temperature has little effect on average micelle size. A higher rotor speed was used to characterize the slower sedimenting species (Fig. 2B). The total baseline adjusted A_{280} is ≈0.04 at 10 s^*. The lack of a plateau >10 s^* is consistent with a reversible association between the slower sedimenting material and the micellar material. The slower boundary moves at $s_{20,w} \approx 3.1$, consistent with the sedimentation coefficient expected for a spherical monomer. The upper limit to the cmc is ≈3 μM under these conditions.

Sedimentation equilibrium analysis showed that any thermal effects on aggregation were fully reversible: MyoD incubated at 40°C for 30 min and MyoD held at 4°C prior to analysis at 23.3°C yielded results identical to those shown in Table 1.

By using 50 s as the sedimentation coefficient of the "average" MyoD aggregate and assuming $M_r = 4.1 \times 10^6$, the micelles model as prolate ellipsoids with an axial ratio ≈ 15, assuming a hydration of 0.3 g of H_2O per g of protein (26).

The Effect of E47-96 on MyoD. MyoD binds to DNA as a heterooligomer with E12 or E47 (13). A 96-residue bHLH fragment of E47 (E47-96) was analyzed since purified full-length E47 was not available. Sedimentation equilibrium analysis reveals that E47-96 exists as a stable homodimer (Table 1).

When equimolar mixtures of full-length MyoD and E47-96 are examined by sedimentation equilibrium (Table 1), the observed molecular weight is within 3% of that expected for a 1:1 complex. Mixtures that underwent a 30-min preincubation

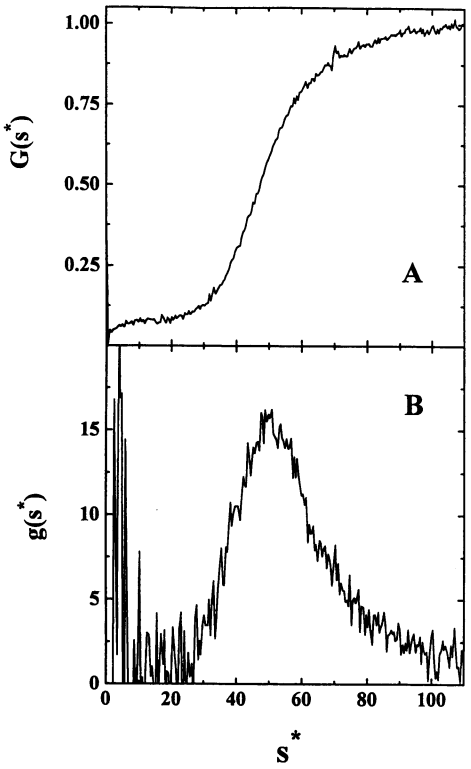

FIG. 1. Sedimentation coefficient distribution functions for full-length MyoD at 20°C. (*A*) Integral distribution function obtained at 20,000 rpm and at an initial concentration of 0.582 A_{280} (12-mm pathlength). Data shown are from a single scan with the radial axis transformed to an apparent sedimentation coefficient (s^*) using $s^* = \ln(r/r_m)/\int\omega^2 dt$, where r_m is the meniscus position and $\int\omega^2 dt$ is the reduced sedimentation time. The *y* axis is the ratio of the absorbance at any radial position to the absorbance in the plateau. For these data, the average absorbance of 15 data points in the region between 90 and 95 *s* was used to calculate the plateau absorbance. (*B*) Differential distribution function calculated from four sequential scans, 2 min apart and at 20,000 rpm. Data are truncated at 10 s^*, where the distribution function becomes excessively noisy due to the inclusion of $1/s^*$ in the calculation of $g(s^*)$ (29).

at 40°C were compared with mixtures that were held at 4°C. Initially, nonpreincubated samples exhibited substantial fringe displacement at 2200 rpm, whereas the preincubated samples did not. After 8 h, neither sample showed any fringe displacement at 2200 rpm, and identical results were obtained at higher rotor speeds. This suggests that elevated temperature affects the kinetics of micelle dissolution but not the final equilibrium with E47-96. Samples containing a 2:1 mole ratio of full-length MyoD to E47-96, both with and without preincubation at 40°C, were also examined. In these cases, stable aggregates ($M_r \approx 4 \times 10^6$) were observed even after 12 h of sedimentation at 2400 rpm. Likewise, the 1:1 complex of full-length MyoD–E47-96 was observed at higher rotor speeds. These results demonstrate that heterodimer formation is a mass-action process and that E47-96 does not somehow "catalyze" the dissolution of the micelles. Sedimentation-velocity analysis was consistent with these observations, revealing both a fast and a slow sedimenting boundary (data not shown).

The HLH domain of MyoD is responsible for heterodimer formation. Previous work demonstrated that MyoD-bHLH exists as a dimer/tetramer equilibrium controlled by a $K_d \approx 17$ μM (16, 30). The M_z of an equilimolar mixture of MyoD-bHLH and E47-96 (Table 1) is near that anticipated for a 1:1 complex of MyoD-bHLH and E47-96, demonstrating that the MyoD-bHLH–E47-96 heterodimer is considerably more stable than at least one of the homodimers.

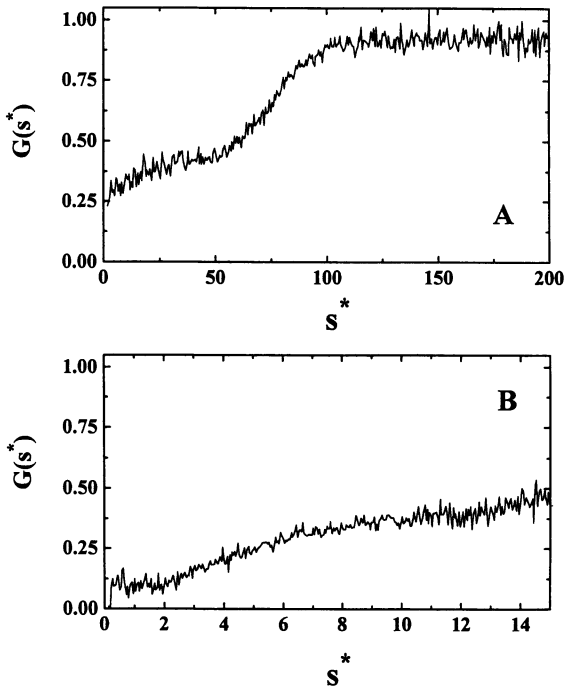

FIG. 2. Integral sedimentation coefficient distribution functions for full-length MyoD at 36°C and at an initial concentration of 0.176 A_{280} (12-mm pathlength). (*A*) Data acquired at 10,000 rpm showing the faster sedimenting material. (*B*) Data acquired several minutes after accelerating the rotor to 48,000 rpm shows the slower sedimenting boundary.

DISCUSSION

The Aggregates of MyoD as Micelles. Micelles are composed of subunits in a reversible, highly cooperative equilibrium with monomers. Because of the cooperativity, there are relatively few species with sizes between the monomer and the micelle, and a cmc is observed. The cmc is constant for a given set of conditions (temperature, pressure, and the concentrations of other components) but can vary if the conditions are changed. At concentrations below the cmc, no micelles are apparent. Above the cmc, nearly all additional material is present as micelles, and the concentrations of all smaller species are almost constant.

A review of the results demonstrates that MyoD exhibits micellar behavior, with extreme cooperativity, a high degree of polymerization, and a reversible equilibrium with monomer. The presence of other small oligomers of MyoD—e.g., dimer, trimer, etc.—cannot be excluded by our data, and the sum of their concentrations is reported as the cmc. Thermodynamically, it is the free monomer concentration that describes the cmc. Thus, the cmcs reported here are upper estimates.

Further evidence of micelle formation is provided by size-exclusion chromatography (results not shown). Full-length MyoD, analyzed at a loading concentration of ≈175 μM, yields a peak at a size >660 kDa, followed by a long plateau and a second peak at about the size of a dimer or tetramer. All of the fractions, including the largest forms of MyoD, could bind specifically and at about the same specific activity to the muscle creatine kinase gene enhancer. Rechromatography of either the larger form or the smaller form of MyoD (brought to the same initial concentration) generated the same column profile. This demonstrates the reversibility of the equilibrium (31, 32). A 68-residue bHLH fragment of MyoD (MyoD-bHLH), purified from bacteria, exhibits only the smaller form of MyoD when analyzed at comparable concentrations. Full-length *in vitro* translated E47 (22), the heterodimeric partner of MyoD, displays behavior similar to that of full-length MyoD, with

species as large as that for MyoD, a lagging shoulder, and a smaller, presumably dimeric species (data not shown).

Consequences of Micelle Formation on MyoD-Dependent Activities. Micelle formation will affect the interactions of MyoD with other macromolecules, primarily due to the near constancy of free monomeric MyoD. Three models are presented in Table 2 that consider the consequences of micelle formation. For simplicity and to indicate the generality of the results, a boldface letter **A** has been substituted for MyoD in the table. Only cases in which the concentrations exceed the cmc are considered.

Model I describes the behavior expected for MyoD itself. Since MyoD binds to DNA as a homodimer, the model considers both dimer and micelle formation. Extension of the model to include other small oligomeric forms is straightforward. The concentration of dimers is constant and depends only on the ratio of the cmc to the dimer dissociation constant. On the other hand, the concentration of micelles depends strongly on the total concentration of MyoD. Therefore, any change that affects the cmc would have a strong effect on the dimer concentration. Such changes could occur in a number of ways—e.g., protein phosphorylation, ligand binding, etc. Any change that reduces the cmc will reduce the dimer concentration by sequestering MyoD in micelles, whereas changes that increase the cmc would mobilize large quantities of MyoD dimers. Such an effect may account for the observed stimulation of DNA binding by MyoD–E47 heterodimers in the presence of cell extracts (18).

Because the concentration of MyoD dimer is constant, the fraction of DNA sites occupied by MyoD also is constant and dependent on the ratio of the cmc to the K_d of the dimer DNA complex (Table 2). This provides a simple mechanism for permitting the binding of MyoD to one site on DNA, while preventing binding at different site. Consider an example with MyoD having a cmc of 10^{-7} M binding nonspecifically to DNA with a K_d of 10^{-5} and to a specific site with a K_d of 10^{-9}. At all concentrations of MyoD exceeding the cmc, the specific site would be 99% filled, while less than 1% of the nonspecific sites would ever fill.

The fact that MyoD forms heterodimers with other HLH-containing proteins is taken into consideration in model II in which a second protein is included (Table 2). In this model, the

Table 2. Consequences of micelle formation at concentrations of proteins above the cmc

Model	Relevant equations	Consequences
I. Single protein **A**. **A** forms dimers and micelles. The dimer binds to a site on DNA.	$[\mathbf{A}_2] = \frac{\mathrm{cmc}_A^2}{K_{d_{A2}}}$ and $[\mathbf{A}_m] = \frac{[\mathbf{A}_2 - \mathrm{cmc}_A]^m}{K_m}$	$[\mathbf{A}_2]$ constant, sensitive to cmc_A; $[\mathbf{A}_m]$ increases rapidly with $[\mathbf{A}_t]$; and for binding of $\mathbf{A}_2$ to a site on DNA with dissociation constant $K_{d_{DNA}}$, the ratio of occupied to unoccupied sites is $\frac{[\mathbf{A}_2\cdot\mathrm{DNA}]}{[\mathrm{DNA}]} = \frac{\mathrm{cmc}_A^2}{K_{d_{DNA}}\cdot K_{d_{A2}}}$.
II. Two proteins **A** and **B**. Both **A** and **B** form dimers and micelles. All dimeric forms compete for a site on DNA.	$[\mathbf{A}_2] = \frac{\mathrm{cmc}_A^2}{K_{d_{A2}}}$, $[\mathbf{B}_2] = \frac{\mathrm{cmc}_B^2}{K_{d_{B2}}}$, $[\mathbf{AB}] = \frac{\mathrm{cmc}_A\cdot\mathrm{cmc}_B}{K_{d_{AB}}}$, and $\frac{[\mathbf{AB}]}{[\mathbf{A}_2]} = \frac{\mathrm{cmc}_B\cdot K_{d_{A2}}}{\mathrm{cmc}_A K_{d_{AB}}}$	$[\mathbf{A}_2]$ constant and independent of **B**; $[\mathbf{B}_2]$ constant and independent of **A**; If both $\mathbf{A}_2$ and $\mathbf{B}_2$ bind to the same site on DNA, the ratio of site occupancy by the two is constant and dependent on the cmc for each protein, as well as the dissociation constants from the DNA site: $\frac{[\mathbf{B}_2\cdot\mathrm{DNA}]}{[\mathbf{A}_2\cdot\mathrm{DNA}]} = \frac{\mathrm{cmc}_B^2}{\mathrm{cmc}_A^2}\cdot\frac{K_{d_{A2\cdot DNA}}\cdot K_{d_{A2}}}{K_{d_{B2\cdot DNA}}\cdot K_{d_{A2}}}$. For heterodimer formation, $[\mathbf{AB}]$ constant and independent of $[\mathbf{A}_t]$ or $[\mathbf{B}_t]$. The ratio of $[\mathbf{AB}]$ to $[\mathbf{A}_2]$ occupancy of a site on DNA is $\frac{[\mathbf{AB}\cdot\mathrm{DNA}]}{[\mathbf{A}_2\cdot\mathrm{DNA}]} = \frac{\mathrm{cmc}_B}{\mathrm{cmc}_A}\cdot\frac{K_{d_{A2\cdot DNA}}\cdot K_{d_A}}{K_{d_{AB\cdot DNA}}\cdot K_{d_A}}$. Similarly, for $[\mathbf{AB}\cdot\mathrm{DNA}]/[\mathbf{B}_2\cdot\mathrm{DNA}]$, $\frac{[\mathbf{AB}\cdot\mathrm{DNA}]}{[\mathbf{B}_2\cdot\mathrm{DNA}]} = \frac{\mathrm{cmc}_A}{\mathrm{cmc}_B}\cdot\frac{K_{d_{B2\cdot DNA}}\cdot K_{d_B}}{K_{d_{AB\cdot DNA}}\cdot K_{d_B}}$.
III. Two proteins **A** and **B**. **A** forms dimers and micelles and **B** forms only dimers.	$[\mathbf{AB}] = \frac{\mathrm{cmc}_A\cdot\left(\frac{[\mathbf{B}_t] - [\mathbf{B}]^2}{K_{d_{B2}}}\right)}{K_{d_{B2}}}$; $[\mathbf{AB}] = \frac{K}{(1+K)}\cdot[\mathbf{B}_t]$, where $K = \frac{\mathrm{cmc}_A}{K_{d_{AB}}}$; and $\frac{[\mathbf{AB}]}{[\mathbf{A}_2]} = \frac{[\mathbf{B}_t]\cdot K_{d_{AB}}}{\mathrm{cmc}_A^2 + \mathrm{cmc}_A\cdot K_{d_{AB}}}$	$[\mathbf{AB}]$ depends only on $[\mathbf{B}]$ and if $K_{d_{B2}} >> [\mathbf{B}_t]$, both $[\mathbf{AB}]$ and $[\mathbf{AB}]/[\mathbf{A}_2]$ vary linearly with $[\mathbf{B}_t]$.

The nomenclature is as follows: **A** and **B** are proteins with [**A**] and [**B**] their monomer concentrations, $[\mathbf{A}_2]$ and $[\mathbf{B}_2]$ their dimer concentrations, and $[\mathbf{A}_m]$ and $[\mathbf{B}_m]$ their micelle concentrations. The total concentrations of all species of **A** and **B** are $[\mathbf{A}_t]$ and $[\mathbf{B}_t]$, respectively. $[\mathbf{AB}]$ is the concentration of a 1:1 complex of **A** and **B**. The dissociation equilibrium constant (dimer ↔ monomer) for $\mathbf{A}_2$ is $K_{d_{A2}}$, for $\mathbf{B}_2$ is $K_{d_{B2}}$, and for the **AB** heterodimer is $K_{d_{AB}}$. The micelle dissociation equilibrium constant (micelle ↔ monomer) for $\mathbf{A}_m$ is K_m (a similar equation applies to the dissociation of $\mathbf{B}_m$). The critical micelle concentrations for **A** and **B** are cmc_A and cmc_B, where the cmc $\approx K_m^{1/(m-1)}$ for micelles containing **m** monomers. The concentration of unoccupied binding sites on DNA is [DNA], and the concentrations of various complexes of dimeric proteins with sites are denoted as $[\mathbf{A}_2\cdot\mathrm{DNA}]$, $[\mathbf{B}_2\cdot\mathrm{DNA}]$, and $[\mathbf{AB}\cdot\mathrm{DNA}]$, with dissociation equilibrium constants of $K_{d_{A2\cdot DNA}}$, $K_{d_{B2\cdot DNA}}$, and $K_{d_{AB\cdot DNA}}$, respectively.

second protein homodimerizes and forms micelles. These characteristics may mimic the behavior of E47. As is shown in Table 2, homodimer formation for the two proteins is completely independent of their heteroassociation properties due to the buffering afforded by micelles. More generally, the independence of all interactions involving smaller oligomers of either protein can be shown. Thus, micelle formation provides a simple mechanism for uncoupling interactions from one another.

In model II, the formation of heterodimer depends on the cmc for each protein but is independent of the homodimer associations and insensitive to the total concentration of either protein (Table 2). Changes in the cmc of either protein will directly affect heterodimer formation. Again, because of the buffering properties of the micelles, the ratios of the concentrations of the various dimeric species are fixed at values specified by the cmcs and K_ds. Therefore, the ratios of the species competing for binding to sites on DNA will be constant and dictated by the cmcs and K_ds (Table 2). On the other hand, changes in the cmcs could adjust these ratios so that either the homodimer or the heterodimer would dominate the binding at a site.

The case in which only one of the two proteins forms micelles is considered in model III. Because protein **B** is not "buffered" by micelle formation, all of the interactions remain dependent on $\mathbf{B}_z$. If **B** dimerizes strongly, then the concentration of the heterodimer is dependent on $K_{d_{B2}}$ and the concentration of **AB** will increase gradually until [**B**] approaches $K_{d_{B2}}$. On the other hand, if dimerization is sufficiently weak, the concentration of **AB** will vary linearly with the total concentration of **B** until the micelles of **A** are depleted. Similarly, the ratio of $[\mathbf{AB}]/[\mathbf{A}_2]$ will vary linearly with $\mathbf{B}_t$ and the ratio of the site occupancy on DNA will depend linearly on $\mathbf{B}_t$.

In general, the degree of cooperativity will depend exponentially on the number of subunits in a complex. Therefore, model II and model III are not completely independent. Rather, they describe limits for how MyoD will behave in heteroassociating systems. In model II, the conjugate protein exhibits the same sort of highly cooperative association behavior as MyoD, whereas in model III, the conjugate protein can show little or no cooperative behavior. This leads to very different expectations concerning concentration dependence of the functions associated with these proteins.

The models described here can be extended to accommodate more proteins and more interactions. This will be needed to describe all of the suspected interactions between MyoD, the various E2A proteins, and MyoD and either Id1 or Id2 (2, 5, 19, 30, 33). Taken together, micelle formation suggests mechanisms in which combinatorial processes could be accommodated by the appropriate adjustment of cmcs and K_ds for such proteins.

Earlier studies involving the bHLH domain of MyoD indicated that this region forms dimers and tetramers, but no evidence of micelle formation was observed (16, 34). Furthermore, a single-site mutation in the loop region of MyoD-bHLH produces a peptide that exhibits micellar behavior, suggesting that fairly small changes can induce the bHLH domain to become micellar (T.M.L., M.A.S., H.W., and R.E.K., unpublished data). However, the structural changes that result in switching from a dimeric to a micellar form are unclear at this time.

The *in vivo* concentration of MyoD is not known. Both the observed localization of MyoD to the nucleus (15) and the nonideality due to macromolecular crowding in this environment (35) would be expected to enhance micellization. Indeed, the punctate staining of nuclei observed by immunofluorescence is consistent with MyoD micellization (15). While the temperature seems to have a minimal effect on the cmc, other factors such as pH, ionic strength, covalent modification, or ligand binding may have larger effects. Thus, it is impossible to predict with certainty whether or not MyoD micelles are formed *in vivo* or which solution properties might regulate micellization. Nevertheless, micelle formation should be kept in mind both when studying the protein *in vitro* and when forming hypotheses concerning its biological function and regulation *in vivo*.

We dedicate this paper to the memory of Hal Weintraub. Support for this project came from the Muscular Dystrophy Association, an American Heart Association Established Investigator Award, and National Institutes of Health Grant RO1GM46701 (to R.E.K.); a National Institutes of Health Molecular Biophysics Training Grant (to M.A.S.); National Science Foundation Grants DIR 891457, DIR 9002027, and BIR 9314040 (to T.M.L.); National Cancer Institute Grant R35-CA42506-08 and National Institutes of Health Grant GM 26176-15 (to H.W.); and Muscular Dystrophy Association (to X.-H.S.). H.W. was an investigator at the Howard Hughes Medical Institute. This is scientific contribution no. 1926 from the New Hampshire Agricultural Experiment Station.

1. Murre, C., McCaw, P. S. & Baltimore, D. (1989) *Cell* **56,** 777–783.
2. Murre, C., McCaw, P. S., Vassin, H., Caudy, M., Jan, L. Y., Jan, Y. N., Cabrera, C. V., Buskin, J. N., Hauschka, S. D., Lassar, A. B., Weintraub, H. & Baltimore, D. (1989) *Cell* **58,** 537–544.
3. Davis, R. L., Cheng, P.-F., Lassar, A. B. & Weintraub, H. (1990) *Cell* **60,** 733–746.
4. Church, G. M., Ephrussi, A., Gilbert, W. & Tonegawa, S. (1985) *Nature (London)* **313,** 798–801.
5. Blackwell, T. K. & Weintraub, H. (1990) *Science* **250,** 1104–1110.
6. Voronova, A. & Baltimore, D. (1990) *Proc. Natl. Acad. Sci. USA* **87,** 4722–4726.
7. Ferré-D'Amaré, A. R., Prendergast, G. C., Ziff, E. B. & Burley, S. K. (1993) *Nature (London)* **363,** 38–45.
8. Ferré-D'Amaré, A. R., Pognonec, P., Roeder, R. G. & Burley, S. K. (1994) *EMBO J.* **13,** 180–189.
9. Ellenberger, T., Fass, D., Arnaud, M. & Harrison, S. C. (1994) *Genes Dev.* **8,** 970–980.
10. Ma, P. C. M., Rould, M. A., Weintraub, H. & Pabo, C. O. (1994) *Cell* **56,** 777–783.
11. Weintraub, H. (1993) *Cell* **75,** 1241–1244.
12. Lassar, A. B. & Munsterberg, A. (1994) *Curr. Opin. Cell Biol.* **6,** 432–442.
13. Lassar, A. B., Davis, R. L., Wright, W. E., Kadesch, T., Murre, C., Voronova, A., Baltimore, D. & Weintraub, H. (1991) *Cell* **66,** 305–315.
14. Kadesch, T. (1993) *Cell Growth Differ.* **4,** 49–55.
15. Tapscott, S. J., Davis, R. L., Thayer, M. J., Cheng, P.-F., Weintraub, H. & Lassar, A. B. (1988) *Science* **242,** 405–411.
16. Starovasnik, M. A., Blackwell, T. K., Laue, T. M., Weintraub, H. & Klevit, R. E. (1992) *Biochemistry* **31,** 9891–9903.
17. Farmer, K., Catala, F. & Wright, W. E. (1992) *J. Biol. Chem.* **267,** 5631–5636.
18. Thayer, M. J. & Weintraub, H. (1993) *Proc. Natl. Acad. Sci. USA* **90,** 6483–6487.
19. Lassar, A. B., Buskin, J. N., Lockshon, D., Davis, R. L., Apone, S., Hauschka, S. D. & Weintraub, H. (1989) *Cell* **58,** 823–831.
20. Davis, R. L., Weintraub, H. & Lasser, A. B. (1987) *Cell* **51,** 987–1000.
21. Studier, F. W. & Moffatt, B. A. (1986) *J. Mol. Biol.* **189,** 113–130.
22. Studier, F. W. (1991) *J. Mol. Biol.* **219,** 27–44.
23. Yphantis, D. A. (1960) *Ann. N. Y. Acad. Sci.* **88,** 586–601.
24. Laue, T. M. (1992) in *Analytical Ultracentrifugation in Biochemistry and Polymer Science*, eds. Harding S. E., Rowe A. J. & Horton J. C. (R. Soc. Chem., Cambridge, U.K.), pp. 63–89.
25. Laue, T. M. (1995) *Methods Enzymol.* **259,** 427–452.
26. Laue, T. M., Shah, B., Ridgeway, T. M. & Pelletier, S. L. (1992) in *Analytical Ultracentrifugation in Biochemistry and Polymer Science*, eds. Harding S. E., Rowe A. J. & Horton J. C. (R. Soc. Chem., Cambridge, U.K.), pp. 90–125.
27. McMeekin, T. L., Marshall, K. (1952) *Science* **116,** 142–143.
28. Kharakoz, D. P. (1989) *Biophys. Chem.* **34,** 115–125.
29. Stafford, W. F., III (1992) *Anal. Biochem.* **203,** 295–301.
30. Benezra, R., Davis, R. L., Lockshon, D., Turner, D. L. & Weintraub, H. (1990) *Cell* **61,** 49–59.
31. Cann, J. R. (1970) *Interacting Macromolecules: The Theory and Practice of their Electrophoresis, Ultracentrifugation, and Chromatography* (Academic, New York).
32. Ackers, G. K. (1968) *J. Biol. Chem.* **243,** 2056–2064.
33. Sun, X.-H., Copeland, N. G., Jenkins, N. A. & Baltimore, D. (1991) *Mol. Cell. Biol.* **11,** 5603–5611.
34. Fairman, R., Beran-Steed, R. K., Anthony-Cahill, S. J., Lear, J. D., Stafford, W. F., III, DeGrado, W. F., Benfield, P. A. & Brenner, S. L. (1993) *Proc. Natl. Acad. Sci. USA* **90,** 10429–10433.
35. Zimmerman, S. B. (1993) *Biochim. Biophy. Acta* **1216,** 175–185.